

Extracts of the 2004 Annual Report of the (former) JGU “Institute of Nuclear Chemistry”

Separation of ^{211}Pb with ALOHA and subsequent electrochemical deposition *Page 2*

H. Hummrich, F. Freist, D. Liebe, J.V. Kratz

Separation of fission products with ALOHA and subsequent electrochemical deposition *Page 3*

H. Hummrich, J.V. Kratz, D. Liebe

The electrochemical deposition of Hg on various metal electrodes *Page 4*

H. Hummrich, F. Feist, J.V. Kratz

**Extraction of Gd, Hf, and Tc with the fast continuous liquid-liquid-extraction
System MicroSISAK** *Page 5*

Eberhardt, S. Andersson, C. Ekberg, B. Horn, J.V. Kratz, P. Löb, M. Nilsson, G. Skarnemark, N. Trautmann

**Theoretical Investigation of the Reactivity of MO_4 and the Electronic Structure
of $\text{Na}_2[\text{MO}_4(\text{OH})_2]$, where M = Ru, Os, and Hs (element 108)** *Page 6*

V. Pershina and J.V. Kratz

Search for the “missing” α -decay branch in ^{239}Cm *Page 7*

Z. Qin, D. Ackermann, W. Bröchle, F.P. Hessberger, E. Jäger, P. Kuusiniemi, G. Münzenberg, D. Nayak, E. Schimpf, M. Schädel, B. Schausten, A. Semchenkov, B. Sulignano, K. Eberhardt, J.V. Kratz, D. Liebe, P. Thörle, Yu.N. Novikov

Further investigations on target preparation for heavy element studies *Page 8*

D. Liebe, P. Thörle, J.V. Kratz

Separation of ^{211}Pb with ALOHA and subsequent electrochemical deposition

H. Hummrich, F. Feist, D. Liebe, J.V. Kratz

Institut für Kernchemie, Johannes Gutenberg-Universität Mainz, Germany

To achieve a fast and (quasi)-continuous transfer of recoil atoms from the recoil chamber into the liquid phase, the ALOHA system was constructed and successfully used in chromatography experiments [1].

To prepare liquid phase experiments with element 114, the separation of its homolog Pb with ALOHA and its subsequent electrochemical deposition was investigated. A ^{219}Rn -emanating source was prepared by co-precipitation of ^{227}Ac with $\text{Fe}(\text{OH})_3$. The source was placed in a 300 ml glass chamber where the 3,96s ^{219}Rn was allowed to decay. The daughter nuclides ^{211}Pb and ^{211}Bi were attached to KCl-clusters and transferred with a He flow of 2 l/min to ALOHA and deposited by impaction on a Ta disc. After impaction, the activity was stepped to the dissolution position and transferred to the electrolytic cell by continuously cyclic pumping of the electrolyte (0.1M HCl) with a low dead-volume HPLC pump. Fig. 1 shows the experimental set-up.

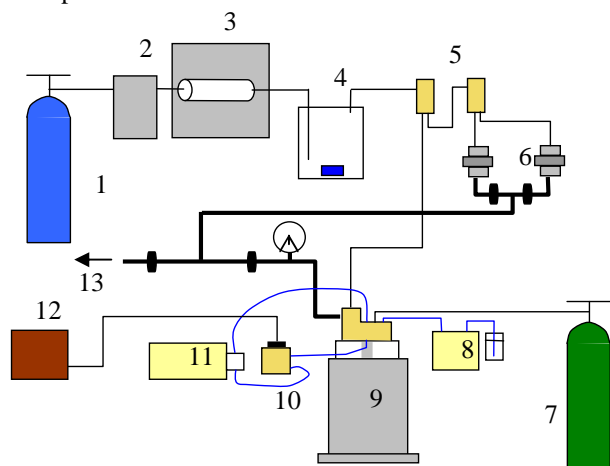


Fig.1: Experimental set-up. 1 Helium, 2 mass-flow-controller, 3 KCl cluster oven, 4 ^{227}Ac emanating source, 5 gas-jet switches, 6 direct catch and waste unit, 7 Nitrogen, 8 Acetone pump, 9 ALOHA, 10 electrodeposition cell, 11 electrolyte pump, 12 potentiostat, 13 to the ventilation system. Gas jet flow: black line, vacuum system: thick black line, liquid flow: blue line

The yield of impaction and dissolution in ALOHA (compared to a direct catch on a glassfiber filter) was measured via γ -spectrometry at different stepping times. Fig.2 shows that about 75 to 90% of the activity was successfully transferred from the gas-jet into the liquid phase using stepping times of 5s and longer. At lower stepping times, activity is lost due to the low dissolution volume.

For electrodeposition experiments with ^{211}Pb , a heatable electrolytic cell was attached to the ALOHA system. Pd was chosen as electrode material, 0.1M HCl as electrolyte. The deposition potential was -500 mV vs. Ag/AgCl.

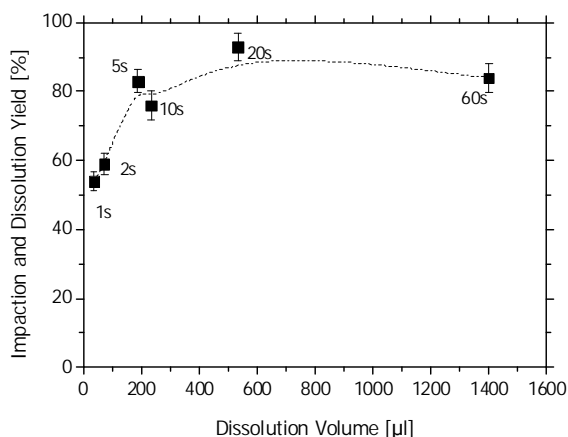


Fig.2: Impaction and dissolution yield for $^{211}\text{Pb}/^{211}\text{Bi}$ vs. dissolution volume (stepping time) with the ALOHA system, solvent 0.1M HCl

The activity was impacted for 10 min in the collection position, transferred to the dissolution position and dissolved. The deposition experiments were carried out at a temperature of ca. 75° and under vigorous stirring. At $t_{50\%}=20\text{ s}$, 50% of the activity was deposited, as can be seen in Fig.3.

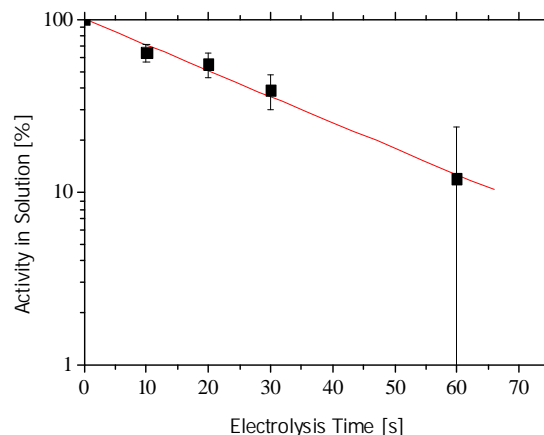


Fig 3: Electrodeposition of ^{211}Pb on Pd electrodes from 0.1M HCl at -500 mV vs. electrolysis time.

The deposited activity could also be measured via α -spectrometry after the radioactive equilibrium between ^{211}Pb and ^{211}Bi was reached. Here, a $0.1\ \mu\text{m}$ polycarbonate filter was used for the direct catch. In both cases, a FWHM of 60 keV for the 6,2 MeV line of ^{211}Bi was achieved

The presented system will be tested in a beam time at GSI with short lived Pb-isotopes in the reaction ^{40}Ar on Gd.

References

[1] A. Kronenberg et al., Annual Report, Institut für Kernchemie, Universität Mainz 2001, A4

Separation of fission products with ALOHA and subsequent electrochemical deposition

H. Hummrich, J.V. Kratz, D. Liebe,

Institut für Kernchemie, Johannes Gutenberg-Universität Mainz, Germany

The separation of fission products was studied with a coupling of the ALOHA system [1] and an electrochemical deposition device. A ^{235}U -Target (see fig. 1), which was covered with $15\ \mu\text{m}$ Al to suppress the heavy-mass fission products, was irradiated at the TRIGA reactor. The light mass fission products recoiling from the target, were stopped in He and transported with a KCl-cluster gasjet to the ALOHA system. After impaction onto a Ta-disc, the disc was stepped into the dissolution position and the fission products were dissolved in 0.1M HClO_4 and transferred into the electrochemical cell by continuously cyclic pumping at a flow rate of $1\text{-}2\ \text{ml/min}$.

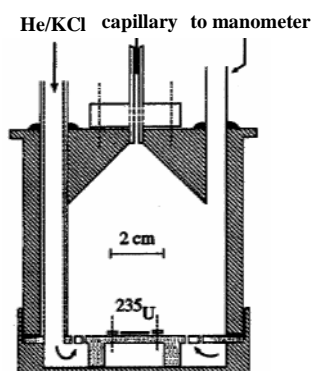


Fig.1: Set-up of the ^{235}U -target and recoil chamber used for fission product production

The overall impaction and dissolution yield in ALOHA compared to a direct catch on a glassfiber filter (measured via the gross γ -activity) was about 80%, if the Ta-disc was stepped in intervals of 5s and longer. For shorter stepping times, the dissolution volume was low compared to the dead volume of the dissolution position, thus leading to a decrease in yield to about 60%. The impaction and dissolution yield for a specific fission product can be determined, if the fractional and the cumulative fission yield are in the same dimension. For ^{84}Se (fractional yield: 0,66%, cumulative yield: 0,99%), $55\pm 10\%$ of the activity was recovered from the gas-jet.

The potential dependence of the electrodeposition yield was investigated. Pd working electrodes and a Pt counter electrode were used. The potential was controlled potentiostatically vs. a Ag/AgCl reference electrode. The fission-products were collected for 5 min., then the electrodeposition was performed for 5 min. at a given potential under vigorous stirring. After that, the deposited activity was measured. The experiment was carried out for various electrode potentials.

Even at -1000mV , only $^{101/104}\text{Tc}$ and ^{84}Se were deposited. ^{101}Mo , ^{93}Sr , ^{90}Rb and ^{94}Y remained in solution. Fig. 2 shows the potentials, at which the electrodeposition of Tc and Se start (critical potential).

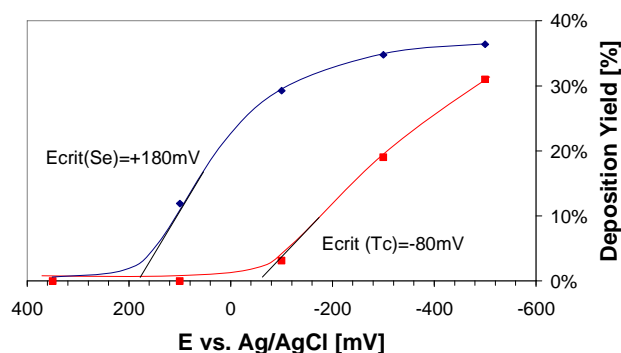


Fig. 2: Critical potentials for the electrochemical deposition of Tc and Se from 0.1M HClO_4 on Pd electrodes

In experiments with fission products with a longer half-life, ^{103}Ru and $^{99\text{m}}\text{Tc}$ could also be electrodeposited onto Pd. At $-500\ \text{mV}$, $^{97/95}\text{Zr}$, ^{96}Nb and ^{99}Mo remained in solution. Fig. 3 shows the critical potential for the deposition of Ru.

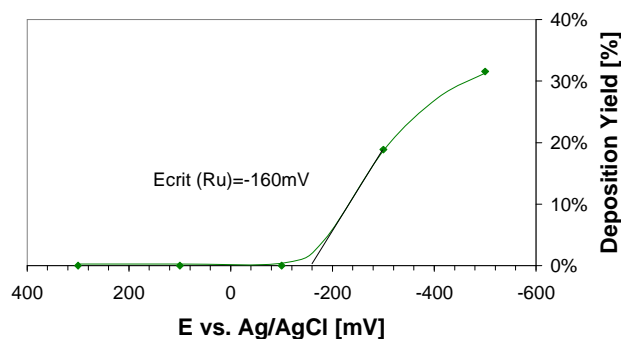


Fig. 3: Critical potential for the electrochemical deposition of Ru from 0.1M HClO_4 on Pd electrodes

In superheavy element chemistry, the coupling of ALOHA with an electrochemical deposition device may be suitable for experiments with Bh (homolog of Tc) and Hs (homolog of Ru). Further experiments with Re and Os, the heavier homologs of Bh and Hs, are necessary to confirm this assumption.

References

[1] H. Hummrich et al., this report

The electrochemical deposition of Hg on various metal electrodes

H. Hummrich, F. Feist, J.V. Kratz

Institut für Kernchemie, Johannes Gutenberg-Universität Mainz, Germany

Recently, attempts were undertaken to chemically characterize element 112 in gas phase experiments [1].

A different approach involves experiments in the liquid phase. If we assume that element 112 is a noble metal (like its homolog Hg), a separation by electrochemical deposition on a metal electrode should be possible. Furthermore, this would result in an ideal sample for α -spectrometry.

In our experiments, we investigated the electrochemical deposition of Hg on various metal electrodes. A solution of $\text{Hg}(\text{NO}_3)_2$ in 0.1M HNO_3 was irradiated at the TRIGA reactor of the Mainz for 6h at a neutron flux of $7 \cdot 10^{11}$ n/s/cm². The isotope ^{197g}Hg with a half live of 64,1h was produced with a specific activity of 70 kBq/mg, and its γ -line at 77 keV was evaluated in the experiments.

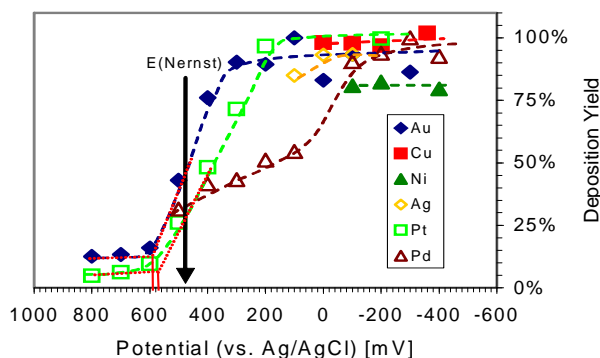


Fig.1: Electrodeposition yield vs. electrode potential for the deposition of ^{197g}Hg on various metal electrodes. In the experiments with Ag, Au, and Cu, 0.1M HNO_3 and with Pt, Pd, and Ni, 0.1M HCl was used as electrolyte

A heatable electrolysis cell with two working electrodes (total area 2 cm²), a Pt counter electrode and a Ag/AgCl reference electrode was used. The electrolyte volume of 1-2 ml was stirred with a high volume magnetic stirrer at 1000-1400 rpm. The total Hg concentration in each experiment was $5 \cdot 10^{-6}$ mol/l. This was low enough, so that the deposition still took place in the sub-monolayer region. 0.1 M HCl and 0.1 M HNO_3 were used as the electrolyte. The electrolysis time was 10 min. This should result in the maximum possible deposition for the given potential.

The electrodeposition yield was measured vs. the electrode potential (Fig. 1). The experiments, in which Ag, Cu, and Ni electrodes were used, were started at the potential that occurred when the electrode is immersed into the solution (rest potential). At the rest potential, no current is applied. An increase of the potential beyond this rest potential would lead to a dissolution of the electrodes. For the deposition of Hg on Pt and Au, a critical potential at which a significant deposition starts, was deduced. For Pd, no well defined critical potential was found. For Cu, Ni, and Ag, the deposition is already nearly complete at the rest potential (spontaneous deposition).

In table 1, the critical potentials are compared with $E_{50\%}$ -values, which were calculated with a microscopic-macroscopic model proposed by Eichler and Kratz [2] using thermodynamic properties of Hg and of the electrode material.

Table 1: Critical potentials for the deposition of Hg on various metal electrodes compared with theoretically predicted $E_{50\%}$ -values (all potentials vs. Ag/AgCl)

Electrode	E_{crit} [mV]	$E_{50\%}$ calc.
Au	+ 600	+ 710
Ni	> +50	+ 660
Ag	> +100	+ 620
Cu	> -100	+ 630
Pt	+ 580	+ 970
Pd	-	+ 1140

The electrodeposition speed was investigated for the deposition on Pd (20° and 80°) and Cu electrodes. Fig. 2 shows the decrease in activity vs. the electrolysis time. The $t_{50\%}$ -value is the time at which 50% of the activity is deposited. The electrodeposition seems to be faster on Cu electrodes than on Pd electrodes at room temperature. An increase in temperature lead to an increase in electrodeposition speed, in analogy to previous experiments with Pb [3].

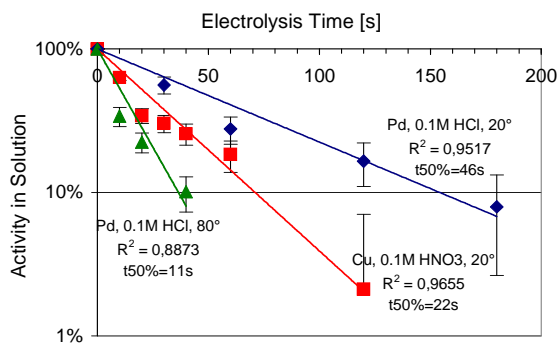


Fig.2: Electrodeposition speed vs. electrolysis time for the deposition of ^{197g}Hg on Pd and Cu. Electrolytic systems: Pd / 0.1M HCl / 20° / -500mV; Cu / 0.1M HNO_3 / 20° / -300mV; Pd / 0.1M HCl / 80° / -500mV

The obtained results will be taken into account in a beam time at GSI, where carrier-free Hg isotopes are produced via the reaction of ^{40}Ar with Sm. The transport of Hg with a KCl gas jet, the transfer into the liquid phase with the ALOHA system [4] and a subsequent electrodeposition will be investigated.

References

- [1] S. Soverna et al, GSI, *Scientific Report 2003*, p. 187
- [2] B. Eichler, J.V. Kratz, *Radiochimica Acta* **88**, 475 (2000)
- [3] H. Hummrich et al., GSI, *Scientific Report 2003*, p. 199
- [4] H. Hummrich et al, *this report*

Extraction of Gd, Hf, and Tc with the fast and continuous liquid-liquid-extraction System MicroSISAK

K. Eberhardt¹, S. Andersson², C. Ekberg², B. Horn³, J.V. Kratz¹,
P. Löb³, M. Nilsson², G. Skarnemark², N. Trautmann¹

¹ Institut für Kernchemie, Universität Mainz, D-55099 Mainz, Germany; ² Chalmers University of Technology, S-41296 Göteborg, Sweden; ³ Institut für Mikrotechnik Mainz, D-55133 Mainz

MicroSISAK is a miniaturized apparatus developed for performing fast and continuous liquid-liquid separations. It is designed to provide a separation time of about 1 s at a flow rate of 60 ml/h (\cong 0.02 ml/s), as required, e.g., for chemical studies of the heaviest elements or for process studies with new types of ligands that are only available in very small amounts. MicroSISAK consists of a stack of microstructured [1] discs with a diameter of 8 mm made of Ti and sealed in a Ti-housing. The main components are:

1. a micromixer (Fig. 1a) with interdigital channels for intense mixing of the phases. Here, small droplets are formed with typical diameters in the range of the channel dimension (see Table 1 for details) yielding an emulsion. The emulsion is subsequently fed into
2. up to three filter units (teflon membrane, 0.5 μ m pore size) for phase separation, as shown in Fig. 1b. A differential pressure Δp (10-50 mbar) regulated via a valve must be applied across the membrane in order to ensure proper phase separation [2].

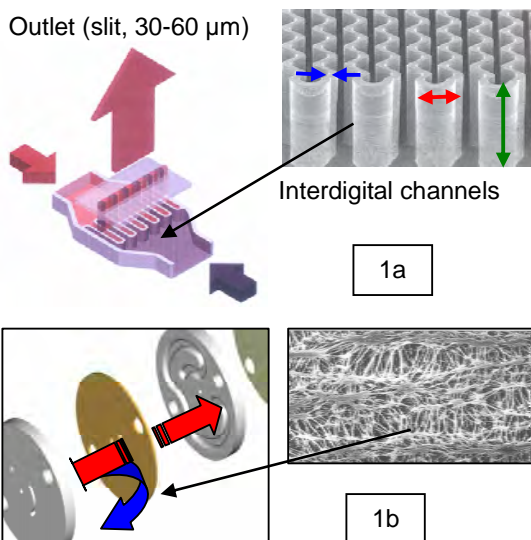


Figure 1: Mixer (Fig. 1a) and filter unit (Fig. 1b) for MicroSISAK. Different mixer types are used (see table 1).

The MicroSISAK set-up has been applied for extraction studies with Gd, Hf, and Tc. Here, different types of mixers have been used in order to optimize the extraction efficiency. Table 1

gives the dimensions of the different types of mixers.

Table 1: Dimensions of the mixer units as used for MicroSISAK (see also Fig. 1a)

Type	Channels	Width	Height	Wall
A	2 x 16	45 μ m	100 μ m	60 μ m
B	2 x 15	30 μ m	100 μ m	60 μ m
C	2 + 1	30 μ m	100 μ m	60 μ m

Figure 2 comprises the results for the extraction of Gd, Hf, and Tc with MicroSISAK. Extraction yields and phase purities have been determined by means of γ -ray spectroscopy. For this, aliquots of the outgoing phases were measured after neutron activation at the TRIGA Mainz. ^{99m}Tc-activity was obtained by milking a commercial Mo-generator. To monitor phase purity, Na₂CO₃ was added to the aqueous phase prior to extraction. The yield depends on the extraction kinetics, the flow rate (hold-up time), and the mixer structure (droplet size).

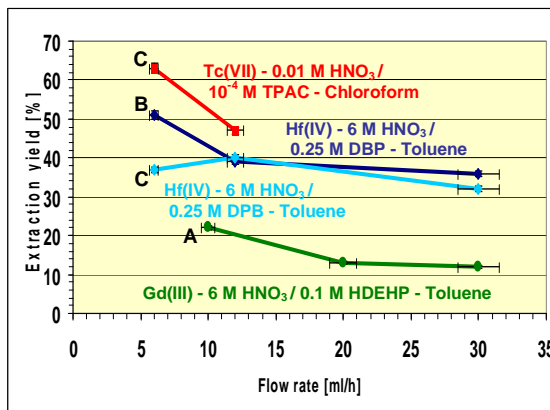


Figure 2: Extraction of Gd, Hf, and Tc with MicroSISAK. A, B, and C indicate the mixer type.

Further experiments are planned to measure the total hold-up time of the system and to optimize the extraction yield for flow rates \leq 60 ml/h (\cong 0.02 ml/s). For this, different combinations of mixer- and filter units will be investigated.

References

- [1] W. Ehrfeld et al., Microreactors, Wiley-VCH Weinheim (2000)
- [2] K. Eberhardt et al., Institut für Kernchemie Annual Report (2003)

Theoretical Investigations of the Reactivity of MO_4 and the Electronic Structure of $\text{Na}_2[\text{MO}_4(\text{OH})_2]$, where $\text{M} = \text{Ru}, \text{Os},$ and Hs (element 108)

V. Pershina* and J. V. Kratz**

*GSI, Darmstadt

**Institut für Kernchemie, Universität Mainz

Recent experiments on the chemical identification of element 108, Hs, have delivered straightforward evidence that it belongs to group 8 of the Periodic Table [1]. In the presence of oxygen, Hs formed HsO_4 which was deposited in a gas-phase chromatography column at a temperature somewhat higher than that of OsO_4 , thus confirming its chemical similarity with the latter and the high volatility. In more recent experiments [2] with volatile tetroxides, HsO_4 was shown to react with moisturized NaOH forming very probably the sodium hassate (VIII), $\text{Na}_2[\text{HsO}_4(\text{OH})_2]$, by analogy with $\text{Na}_2[\text{OsO}_4(\text{OH})_2]$ according to the reaction



In the present work, we study the reactivity of RuO_4 , OsO_4 , and HsO_4 with NaOH on the basis of results of the fully relativistic calculations for the components of the reaction of type (1) using the 4-component Density-Functional Theory method [3]. A model [4] was used to determine the free energy change ΔG^f of a reaction via changes in the ionic (ΔE^C) and covalent (ΔE^{OP}) contributions to the total binding energy. The latter are calculated using Mulliken effective charges Q_M and overlap populations, OP. It was shown that relative values of ΔG^f could be reliably predicted via the ΔE^C . The bond lengths (R_e) of the Os complex were taken from the experiment [5], and those of the Ru and Hs complexes were estimated using R_e for RuO_4 and HsO_4 with respect to $R_e(\text{OsO}_4)$ [6].

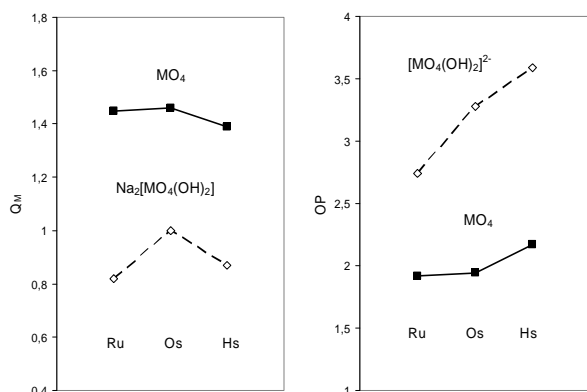


Fig. 1. Effective metal charges, Q_M , and overlap populations, OP, in MO_4 [6] and $[\text{MO}_4(\text{OH})_2]^{2-}$ [this work] ($\text{M} = \text{Ru}, \text{Os},$ and Hs).

The values of Q_M and OP obtained for $[\text{MO}_4(\text{OH})_2]^{2-}$ and MO_4 are depicted in Fig. 1. They show $[\text{HsO}_4(\text{OH})_2]^{2-}$ to be more covalent than the Os homolog, similarly to MO_4 . Both Q_M and OP in $[\text{RuO}_4(\text{OH})_2]^{2-}$ are significantly smaller than Q_M and OP of the Os and Hs anions, which is indicative for

the fact that the Ru anion is not stable due to the weak ionic and covalent constituents of the bond strength. This is not the case with MO_4 , where Q_M and OP of RuO_4 are very similar to those of OsO_4 (Fig. 1).

Table 1. Coulomb binding energies, E^C , for complexes of Ru, Os, and Hs and their differences, ΔE^C (in eV), for reactions of the complex formation

Complex/reaction	Ru	Os	Hs	Ref.
$E^C: \text{MO}_4$	-13.74	-13.86	-12.04	6
$E^C: [\text{MO}_4(\text{OH})_2]^{2-}$	-3.58	-7.64	-5.26	this
$E^C: \text{Na}_2[\text{MO}_4(\text{OH})_2]$	-5.70	-8.77	-6.41	this
$\Delta E^C: \text{MO}_4 \Leftrightarrow [\text{MO}_4(\text{OH})_2]^{2-}$	10.16	6.23	6.78	this
$\Delta E^C: \text{MO}_4 \Leftrightarrow \text{Na}_2[\text{MO}_4(\text{OH})_2]$	8.04	5.09	5.63	this

The obtained E^C for the species and ΔE^C for the complex formation reactions are given in Table 1. The values are similar for reactions of HsO_4 and OsO_4 : HsO_4 should be slightly less reactive than OsO_4 . We can give the upper limit of the difference in ΔG^f between HsO_4 and OsO_4 of 52 kJ/mol defined by the difference in their ΔE^C . (The slightly larger $\Delta \text{OP}=1.42$ for the Hs reaction than $\Delta \text{OP}=1.34$ for the Os reaction should slightly decrease this value). The values of ΔE^C for the reactions of RuO_4 are about 300 kJ/mol more positive than ΔE^C of the OsO_4 and HsO_4 reactions. The reason for that is the too low stability of the Ru complex anion manifested in its low E^C (low Q_M) and low E^{OP} (low OP) (Fig. 1). Thus, the so much more positive ΔG^f of the complex formation reaction of Ru compared to those of Os and Hs explains why $[\text{RuO}_4(\text{OH})_2]^{2-}$ is not known. Finally, on the basis of these calculations, we predict the following trend for the formation of $[\text{MO}_4(\text{OH})_2]^{2-}$, or $\text{Na}_2[\text{MO}_4(\text{OH})_2]$ in group 8:



The predicted slightly lower reactivity of HsO_4 as compared to that of OsO_4 has so far not clearly been revealed experimentally [2].

References

- [1] C. Düllmann *et al.* Nature (Letters) **418**, 859 (2002).
- [2] A. von Zweidorf, *et al.* A. Radiochim. Acta **92**, 855 (2004).
- [3] S. Varga *et al.* Phys. Rev. A **59**, 4288 (1999).
- [4] V. Pershina, Radiochim. Acta **92**, 455 (2004).
- [5] N. N. Nevskii, *et al.* Dokl. Akad. Nauk. **266**, 628 (1982).
- [6] V. Pershina, *et al.* J. Chem. Phys. **115**, 792 (2001).

Search for the "missing" α -decay branch in ^{239}Cm

Z. Qin^{1,2}, D. Ackermann^{1,3}, W. Bröchle¹, F.P. Hessberger¹, E. Jäger¹, P. Kuusiniemi¹, G. Münzenberg¹, D. Nayak^{1,4}, E. Schimpf¹, M. Schädel¹, B. Schausten¹, A. Semchenkov^{1,6}, B. Sulignano^{1,3}, K. Eberhardt³, J.V. Kratz³, D. Liebe³, P. Thörle³, Yu.N. Novikov^{1,5}

¹GSI, Darmstadt, Germany, ²Institute of Modern Physics, Chinese Academy of Science, Lanzhou, P.R. China,

³Johannes Gutenberg-Universität, Mainz, Germany, ⁴Saha Institute of Nuclear Physics, Kolkata, India,

⁵Petersburg Nuclear Physics Institute, Gatchina, Russia, ⁶Technical University of Munich, Germany

It is of special interest to search for those unknown α -emitters in the transuranium region which (i) are located along the path of α -decay chains that start in the super-heavy element region, and (ii) establish a link to nuclides with known masses. The knowledge of all Q_α values in an α -decay chain provides direct information on strongly desired mass values of SHE [1]. A search for the α -decay of ^{239}Cm was carried out at JAERI applying nuclear chemistry techniques [2]. Three α -events with an energy of 6.43 ± 0.14 MeV were assigned to ^{239}Cm and the α/EC branching ratio was estimated as $(6.2 \pm 1.4) \times 10^{-5}$. However, due to this poor statistics, not only the α -energy was determined with an insufficient precision but also the isotope assignment remained questionable.

In our experiment, curium isotopes were produced in the reaction $^{232}\text{Th}(^{12}\text{C},\text{xn})^{244-x}\text{Cm}$. Banana-shaped ^{232}Th targets were prepared by molecular plating at the University of Mainz. As a backing material, 5 μm thick Ti and 15 μm thick Be foils were used. Th target thicknesses were ≈ 700 $\mu\text{g}/\text{cm}^2$ on Ti and ≈ 900 $\mu\text{g}/\text{cm}^2$ on Be. $^{12}\text{C}^{2+}$ beams from the UNILAC were chosen such that after passing through a 20 μm Be vacuum window, He cooling gas of 200 mbar, and the backing material, the ^{12}C projectile energy was 74 MeV in the middle of the target. According to HIVAP calculations, this energy corresponds to the maximum of the excitation function for the reaction $^{232}\text{Th}(^{12}\text{C},5\text{n})^{239}\text{Cm}$. Irradiations were performed with the rotating target wheel ARTESIA. Reaction products recoiling out of the target were implanted into 3.9 μm Cu catcher foils mounted 4 mm behind the rotating target wheel. Most fission fragments passed through the catcher because of their high TKE. To avoid overheating of the target and catcher material by the intensive ion beam, irradiations were carried out in a He atmosphere at 200 mbar. Each irradiation lasted ≈ 6 to 8 hours, and typical (particle) beam intensities varied between 0.3 μA during daytime and 0.85 μA at night. After irradiation, the copper catcher wheel was dismantled and was transported to a chemistry laboratory. The radiochemical separation procedure to prepare a purified Cm sample for α -spectroscopy was finished within 1.5 h or less. This procedure is described in a separate contribution to this report [3].

Two separate runs were carried out at the beginning and end of November. During the first run, targets with Th on Ti were used. They failed because of massive losses of target material from the Ti backing during the irradiation. Furthermore, $^{48,49,51}\text{Cr}$, $^{43,44,46-48}\text{Sc}$, and $^{55,56}\text{Co}$ were produced from ^{12}C on Ti reactions with very high β -

and γ -activities masking complementary γ -spectroscopic measurements. During the second run, targets with Th on Be foil were used which did not show significant Th losses. β and γ activities were about ten times lower than in the first run, and the nuclides mentioned above were not present.

In attempts to identify ^{239}Cm by γ -spectroscopic measurements, some samples were measured with a γ -x-detector and with a Ge-clover detector. γ -ray spectra dominantly showed lines from the decay of ^{153}Sm , $^{150,151}\text{Pm}$ and ^{147}Nd originating from fission of the compound nucleus. Cross sections for these isotopes are about 5 mb [4]. These activities from chemically not separated homologous rare earth elements did not allow identifying ^{239}Cm in the (single) γ -spectra or any Cm by characteristic x-rays. A further evaluation of coincidences is under way.

Samples were assayed for α -activities by 450 mm^2 PIPS detectors. The energy resolution of the evaporated samples was 60 keV. The α -events together with detector numbers and associated times were recorded and stored in list mode. Fig. 1 shows, for the first 10 h measuring time, the sum spectrum of five samples. As expected, ^{240}Cm (4n-channel, $\approx 100\%$ α -decay) with α -energies of 6.29 and 6.24 MeV is dominant. Interestingly, there are some events around 6.5 MeV, close to the energy of ^{238}Cm (6n-channel). Data analysis and search for ^{239}Cm with a reported energy of 6.43 MeV [2] are in progress.

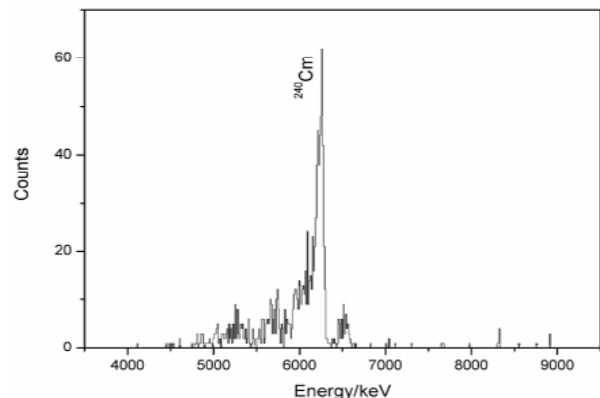


Fig.1 Sum α -spectrum of five samples ($t_m=10$ h each).

- [1] G. Münzenberg, FRS Berichte, GSI (1995) (unpublished)
- [2] N. Shinohara et al., JAERI-Review 2002-029, p. 45
- [3] Z. Qin et al., GSI Scientific Report 2004
- [4] A. Ramaswami et al., J. Radiochem. Nucl. Chem. 246 (2000) 225

Further investigations on target preparation for heavy element studies.

D.Liebe, P.Thörle, J.V. Kratz

Institut für Kernchemie, Universität Mainz, D-55099 Mainz, Germany

For heavy element studies at GSI, again lanthanide and actinide target segments for the rotating wheel assembly were prepared by molecular plating. ^{232}Th targets were used during two ^{12}C beamtimes to investigate the decay of ^{239}Cm [1]. Er has been again by ^{12}C to perform Multi-Column Experiments with Tungsten. The procedures for molecular plating have been applied basically as approved before [2]. Ti with a thickness of $5\mu\text{m}$ has been used as backing for both, Th and Er. Additionally, one target wheel with three segments of Th on an $15\mu\text{m}$ Be-Backing had to be prepared as well since the Th on the Ti-backing was lost almost completely from the rotating wheel during the first beamtime in september 2004. See Table 1.

Table 1: Segments for rotating wheel at GSI

Isotope	Backing	Thickn. [$\mu\text{g}/\text{cm}^2$]
Th	Ti / $5\mu\text{m}$	700
Th	Ti / $5\mu\text{m}$	710
Th	Ti / $5\mu\text{m}$	410
Er	Ti / $5\mu\text{m}$	550
Er	Ti / $5\mu\text{m}$	570
Er	Ti / $5\mu\text{m}$	560
Th	Be / $15\mu\text{m}$	1000*
Th	Be / $15\mu\text{m}$	900
Th	Be / $15\mu\text{m}$	950*

* plated twice

In order to improve the yield and the surface quality of all of those targets numerous tests have been done prior to and after the actual GSI -targets. The use of an ultrasonic probe for cleaning the backing foil prior to deposition seemed to be promising. The optimized parameters are listed below:

Pretreatment:

- washing the already mounted backing with acetone, HCl, H_2O , isopropanol.
- ultrasonic cleaning in isopropanol
- 14 ml fresh and water free isopropanol

Electrodeposition of Th

- 1.0-1.5 ml Th in isopropanol (corresponding to 2mg/ml)
- $10\mu\text{l}$ 0,1n HNO_3
- Voltage 10 min at 0.5 kV, 50min at 1.0kV

Electrodeposition of Er

- $3\text{-}5\mu\text{l}$ Er in 0.1n HNO_3 (corresponding to 200mg/ml)
- Voltage 1.0 kV constantly for 60min

Depositions yields are calculated from neutron activated aliquots of the plating solution prior to and after the procedure.

With ultrasonic treatment, which lasted up to 120min, the foil surfaces looked more structured than without this pretreatment. However, so far, there is no linear dependence of surface stability and deposition yield on the duration of the ultrasonic pretreatment of the Ti or Be backings.

A second issue was to achieve the required target thickness, surface stability and uniformity by two or three subsequent plating procedures. The quantity of Th used for each plating was decreased from 1.5ml to 0.5ml isopropanolic Th-Solution because higher deposition yields at lower concentration seem to be achieved. All other conditions remained as before. In general, the surfaces of all so prepared targets seemed to be more uniform and stable than for targets prepared at once. The densities of multi-plated targets varied between 814–1170 $\mu\text{g}/\text{cm}^2$ what corresponds to a deposition yield of 55–78 %. See table 2.

Table 2: Multi plated targets

Target	1	2	3	4
1.pl. [$\mu\text{g}/\text{cm}^2$]	329	131	285	212
2.pl. [$\mu\text{g}/\text{cm}^2$]	377	233	430	264
3.pl. [$\mu\text{g}/\text{cm}^2$]	310	474	455	338
sum [$\mu\text{g}/\text{cm}^2$]	1016	707	885	602

Backing: Ti $25\mu\text{m}$, other conditions see text.

Besides the target preparation recent work focuses also on requirements of the newly formed TASCAs project. Some basic investigations are already in progress since december 2004. Especially the usability of very thin aluminium ($2\text{-}10\mu\text{m}$) as backing material for uranium deposition takes priority.

References:

- [1] Z. Quin et al., " Search for the 'missing' α -decay branch in ^{239}Cm ", GSI Scientific Report 2005
- [2] K.Eberhardt et al., "Preparation of Targets by electrodeposition for heavy element studies", Nuclear Instruments and Methods in Physics Research A 521 (2004), 208-213